

Wave-like Formation of Hot Loop Arcades

A. Reva¹ · S. Shestov¹ · I. Zimovets² ·
S. Bogachev¹ · S. Kuzin¹

© Springer ●●●

Abstract We present observations of hot arcades made with the Mg XII spectroheliograph onboard the CORONAS-F mission, which provides monochromatic images of hot plasma in the Mg XII 8.42 Å resonance line. The arcades were observed to form above the polarity inversion line between Active Regions NOAA 09847 and 09848 at four successive episodes: at 09:18, 14:13, and 22:28 UT on 28 February 2002, and at 00:40 UT on 1 March 2002. The arcades all evolved in the same way: a) a small flare (precursor) appeared near the edge of the still invisible arcade, b) the arcade brightened in a wave-like manner — closer loops brightened earlier, and c) the arcade intensity gradually decreased in ≈ 1 h. The estimated wave speed was ≈ 700 km s⁻¹, and the distance between the hot loops was ≈ 50 Mm. The arcades formed without visible changes in their magnetic structure. The arcades were probably heated up by the instabilities of the current sheet above the arcade, which were caused by an MHD wave excited by the precursor.

Keywords: Flares, Waves

1. Introduction

It is generally accepted that the energy source of solar flares is the energy of the coronal magnetic field. According to the standard flare model (Carmichael, 1964; Sturrock, 1966; Hirayama, 1974; Kopp and Pneuman, 1976), a magnetic reconnection occurs in the corona. Inside the reconnection region, electrons are accelerated. The accelerated electrons propagate to the lower layers of the solar atmosphere, stop in the chromosphere, heat it, and create hard X-ray (HXR) sources. The heated chromospheric material expands into the corona filling the magnetic field lines with hot and dense plasma. Many flares show signs of the standard model: HXR emission at the loop footpoints and apexes, plasma up-flows inferred from Doppler shifts, and magnetic field configuration highlighted in extreme ultra-violet (EUV) images.

¹ Lebedev Physical Institute, Russian Academy of Sciences
email: reva.antoine@gmail.com

² Space Research Institute, Profsoyuznaya 84/32, Moscow
117997, Russia

Post-flare arcades are a good testing ground for the standard flare model. Whereas arcades are frequently observed with EUV telescopes, a ‘truly hot’ arcade is not as frequent. In fact, the only report we found is given by Warren *et al.* (1999). Slightly more numerous are observations of HXR ribbons in the arcade footpoints (Masuda, Kosugi, and Hudson, 2001; Liu *et al.*, 2007; Jing *et al.*, 2007; Krucker *et al.*, 2011). In all these articles, the authors stressed that the properties of the phenomena under analysis — H_α and HXR ribbons, magnetic reconfiguration, sheared magnetic field, and heating and cooling of plasmas — are consistent with the standard flare model.

The standard flare model is 2D or 2.5D in nature. However, some observations require a 3D explanation; for example, sequential brightening of the flare arcade (Vorpahl, 1976), spreading of heating from a localized flare to a neighboring active region (Parenti, Reale, and Reeves, 2010), HXR footpoint motion along the arcade (Bogachev *et al.*, 2005; Grigis and Benz, 2005), and asymmetric filament eruption (Liu, Alexander, and Gilbert, 2009; Tripathi, Isobe, and Mason, 2006). To further develop a flare theory, we need to extend the standard flare model into 3D.

It is widely accepted that changes in the coronal magnetic structure — flux emergence, flux cancellation, or footpoints shearing motion — may drive flare reconnection (see reviews such as Benz, 2008; Fletcher *et al.*, 2011). However, several authors have proposed that MHD waves can trigger instabilities in the current sheet, which will lead to the reconnection (Vorpahl, 1976; Somov and Syrovatskii, 1982; Nakariakov *et al.*, 2006; McLaughlin, Hood, and de Moortel, 2011; Nakariakov and Zimovets, 2011; Artemyev and Zimovets, 2012).

To observationally investigate flare heating, we need some way to see hot plasma. The most commonly used instruments for hot plasma research — the *Atmospheric Imaging Assembly* (AIA; Lemen *et al.*, 2011) onboard the *Solar Dynamic Observatory* (SDO), the *X-Ray Telescope* (XRT; Golub *et al.*, 2007) onboard *Hinode*, and the *Soft X-ray Telescope* (SXT; Tsuneta *et al.*, 1991) onboard *Yohkoh* — have wide spectral sensitivity. Their images contain cold plasma background, and isolation of hot plasma requires various reasonable assumptions (Reale *et al.*, 2011; Warren, Winebarger, and Brooks, 2012; Testa and Reale, 2012). It would be ideal for flare heating research to obtain monochromatic images of the solar corona in a hot monochromatic line.

In this work, we present the first observations of the formation of hot loop arcades in a hot monochromatic line. The behavior of the observed arcades cannot be explained with the 2.5D standard flare model: they formed in a wave-like manner without changes in their magnetic structure. The aim of this work is to present the observations and give them a reasonable interpretation.

2. Observational Data

We analyzed hot loop arcades observed on 28 February 2002 at 09:18, 14:13, and 22:28 UT and on 1 March 2002 at 00:40 UT. We mainly used the Mg XII spectroheliograph (Zhitnik *et al.*, 2003) data to investigate the behavior of hot arcades, the *Michelson Doppler Imager* (MDI; Scherrer *et al.*, 1995) data to infer

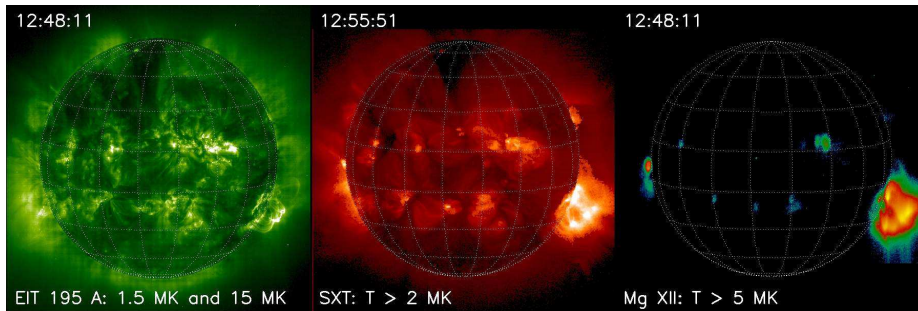


Figure 1. Comparison of hot plasma imagers. Left: EIT 195 Å image, middle: SXT image (AlMg filter), right: Mg XII image. Images were taken on 1 October 2001.

the photospheric magnetic field beneath the arcades, the *Reuven Ramaty High Energy Solar Spectroscopic Imager* (RHESSI; Lin *et al.*, 2002) data to determine where the accelerated particles were present in the arcade, and the *Extreme ultraviolet Imaging Telescope* (EIT; Delaboudinière *et al.*, 1995) data to see how the arcades looked like in low-temperature lines.

The Mg XII spectroheliograph was dedicated for hot plasma observations. It was launched in 2001 onboard the CORONAS-F satellite (Oraevsky and Sobelman, 2002) as a part of the SPIRIT instrumentation complex (Zhitnik *et al.*, 2002). The instrument provides monochromatic solar coronal images in the Mg XII 8.42 Å resonance line. The plasma emits this line at temperatures greater than 5 MK; therefore, the Mg XII images contain only signal from hot plasma without any low-temperature background. Mg XII images differ from other telescopic images — there is neither a solar limb nor a quiet Sun background (see Figure 1). Typical structures in Mg XII images range from 4 to 300 Mm in size and have a lifetime of several seconds up to several days (Urnov *et al.*, 2007). The Mg XII spectroheliograph has two main advantages over ‘traditional’ hot coronal imagers: 1) the entire signal shown in the Mg XII images is from a hot plasma, and 2) faint features can be seen, because no cold background obscure them.

In the present work, we used the Mg XII spectroheliograph data obtained with a 105 s cadence and an 8'' resolution. Due to instrumental effects, Mg XII images are slightly elongated in one of the directions (Reva *et al.*, 2012). We pre-processed the Mg XII data by subtracting the background and removing the signal caused by the radiation damage. To improve the visibility of faint features on the Mg XII images, we used a power scale with index 0.3 (see Figures 1 – 3). In the Mg XII images of Figures 1 – 3, blue and green correspond to low intensities, red and yellow to high intensities.

The MDI onboard the SOHO satellite (Domingo, Fleck, and Poland, 1995), maps the line-of-sight component of the photospheric magnetic field in a synoptic mode with a 4'' resolution and a 90 min cadence.

The RHESSI observes HXR spectra from 3 keV up to 17 MeV. Using Fourier-based methods, RHESSI can synthesize HXR images in the same spectral range. RHESSI data were available for two out of four observed arcades.

The EIT on SOHO satellite takes solar images at the wavelengths centered at 171, 195, 285, and 304 Å. In a synoptic mode, EIT takes images in all four channels every 6 h; in the ‘CME watch’ mode the telescope takes images in the 195 Å channel every 12 min. The pixel size of the telescope is 2.6'' and the spatial resolution is 5''. We used ‘CME watch’ EIT data for auxiliary purposes — to observe the cool plasma. Unfortunately, no H_α images were available for the analyzed arcades.

3. Results

All four hot arcades formed in the same active region (AR), above the polarity inversion line (PIL) between the two elongated regions of opposite polarities (AR NOAA 09847 and 09848; see Figure 2 left). On 25 February 2002, there was a flux emergence in the western part of the negative polarity region, and on 1 March 2002, it disappeared. This flux emergence caused 26 flares, and in four of them we observed the formation of hot loop arcades at 09:18, 14:13, and 22:28 UT on 28 February 2002, and at 00:40 UT on 1 March 2002 (see Figure 3). All four arcades evolved in the same way:

- i) A small hot source, which we call ‘the precursor’, appeared above the flux emergence region in the Mg XII images. At the same place and approximately at the same time, an HXR source appeared in the RHESSI images (see Figure 4). This phase lasted for 2 – 10 min.
- ii) Then, a hot plasma was observed to fill the loops in a wave-like process: the loops that were closer to the precursor structure were filled earlier than the loops that were farther away. All four arcades formed in 5 min, which corresponds to a wave speed of approximately 700 km s⁻¹.
- iii) The emission intensity of the loops increased and reached maximum after 5 - 20 min. The maximum intensity was located in the apex of the loops above the PIL.
- iv) The emission intensity of the loops gradually decreased over approximately 1 h.

Table 1 lists the characteristics of the observed arcades.

All four arcades had similar sizes; the loop length was 170 Mm, and the arcade length was 200 Mm (see Figure 2 center). The arcades consisted of 3 – 5 loops

Table 1. Arcades parameters.

No	Date	GOES class	Precursor start	First loop start	Last loop start	Arcade faded away	Number of loops
1	28 Feb 2002	C4.0	09:20	09:27	09:29	11:20	5
2	28 Feb 2002	C5.5	14:13	14:16	14:20	15:45	3
3	28 Feb 2002	C7.5	22:35	22:40	22:45	23:49	3
4	01 Mar 2002	C3.0	00:37	00:42	00:49	01:33	4

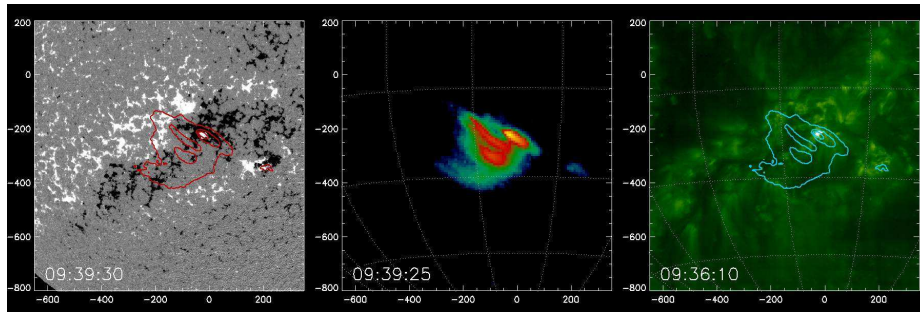


Figure 2. The hot loop arcade of 28 February 2002 at 09:23 UT. Left: MDI image (the movie is available as electronic supplementary material); the red contours denote the Mg XII signal. Middle: Mg XII 8.42 Å image. Right: EIT 195 Å image; the blue contours denote the Mg XII signal. The coordinates are in units of arcsec.

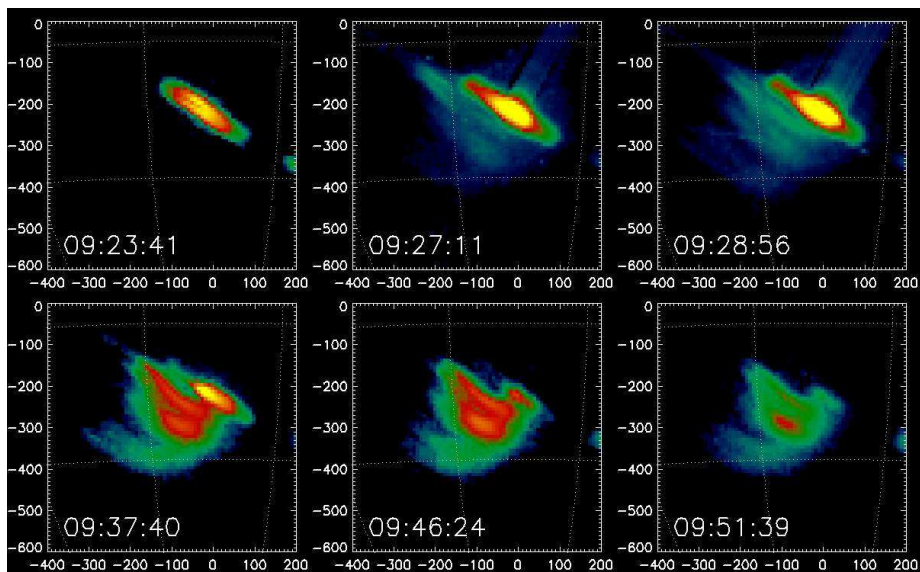


Figure 3. The hot arcade of 28 February 2002 at 09:23 UT; ‘0’ marks the precursor structure and ‘1’ – ‘5’ denote the arcade. The coordinates are in units of arcsec. (A movie is available as electronic supplementary material.)

separated at ≈ 50 Mm. The brightness of the loops gradually decreased with distance from the precursor structure. The loop footpoints were rooted in the main regions of positive and negative polarities (see Figure 3).

In the EIT 195 Å images, the precursor structure looked like a loop with a size of 20 Mm, but the arcade was invisible (see Figure 2 right). When the arcade cooled down and disappeared from the Mg XII images, the brightest loop of the arcade appeared in the EIT 195 Å images.

The HXR source appeared above the flux emergence region at 09:26 and 14:14 UT (events 1 and 2; see Figure 4). There were no other HXR emissions during the events. RHESSI data were unavailable for the other two events. Figure 5 shows RHESSI, GOES, and Mg XII light curves for the arcade that

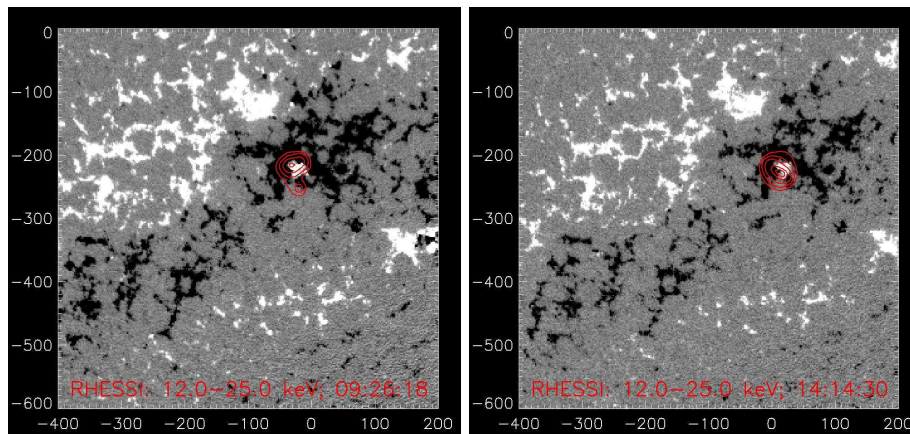


Figure 4. RHESSI HXR sources (contours, reconstructed by the Pixon method) in the 12 – 25 keV spectral range superposed on the MDI magnetogram. The left panel shows the 09:26 UT event, the right panel the 14:14 UT event. There were no RHESSI data for the other two arcades. The coordinates are in units of arcsec.

occurred at 09:26 UT. The majority of the flux in Figure 5 came from the precursor structure. The hard channels peaked earlier than the soft channels (RHESSI: 25 – 50 keV peaked at 09:25:04 UT, 12 – 25 keV at 09:25:32 UT, 6 – 12 keV at 09:26:16 UT; the GOES channels peaked at 09:27:00 UT; and Mg XII peaked at 09:28:56 UT), which is consistent with the standard flare model.

We measured the light curves in the Mg XII 8.42 Å line of the precursor structures and individual loops of the arcades (see Figure 6). The maximum intensity of the precursor structure exceeded the maximum intensity of the brightest loop by one order of magnitude and by two orders of the intensity of the faintest loop. The maximum intensity of the loops exponentially decreased with the distance from the precursor structure (see Figure 7). The intensity e-folding distance is 35 ± 5 Mm.

To measure the plasma cooling time (τ), we approximated the light curves of the precursor structure and the loops by the following formula:

$$I = I_0 e^{-t/\tau}. \quad (1)$$

The cooling time was 4 – 6 min for the precursor structure and 15 – 35 min for the loops (see Table 2). Although it is intuitive to interpret the longer lifetime of the loops as a sign of continuous heating, it is also possible to explain it as a pure cooling (see the Appendix).

4. Discussion

Some aspects of the observed arcades are unusual; the first one is the magnetic configuration in which the events occurred. The precursor occurred above the flux emergence region in a quadrupolar magnetic configuration, suitable for flaring reconnection (see Figure 8). It is clear that the flux emergence caused the

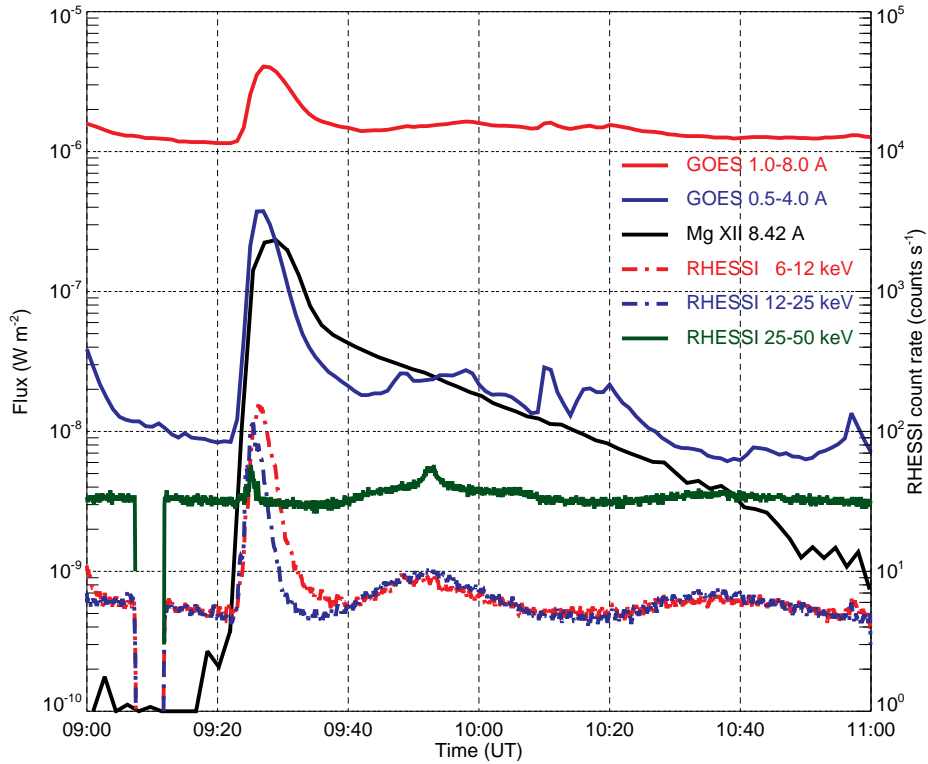


Figure 5. Light curves of the arcade that occurred on 28 February 2002 at 09:23 UT; we indicate the 1 – 8 Å (red) and 0.5 – 4 Å (blue) channels of GOES, Mg XII 8.42 Å (black), 6 – 12 keV (red dash-dotted), 12 – 25 keV (blue dash-dotted), 25 – 50 keV (green) channels of RHESSI.

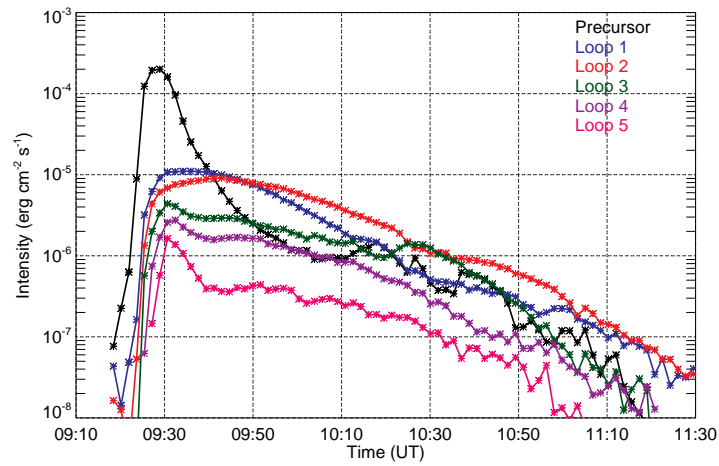


Figure 6. Light curves of the precursor structure and individual loops of the arcade in the Mg XII 8.42 Å line. The arcade occurred after the flare on 28 February 2002 at 09:23 UT. The light curves of other arcades were similar to these curves.

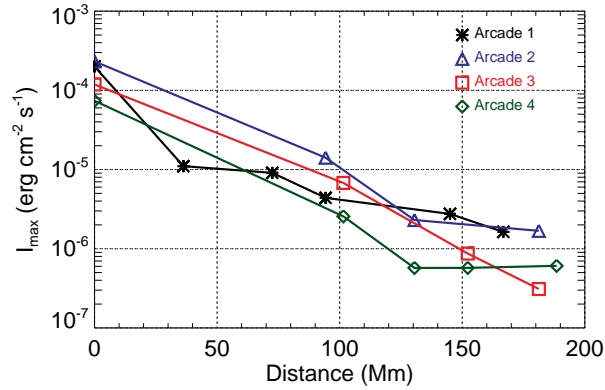


Figure 7. Maximum intensity of the loops observed in the Mg XII 8.42 Å line as a function of the distance from the precursor structure.

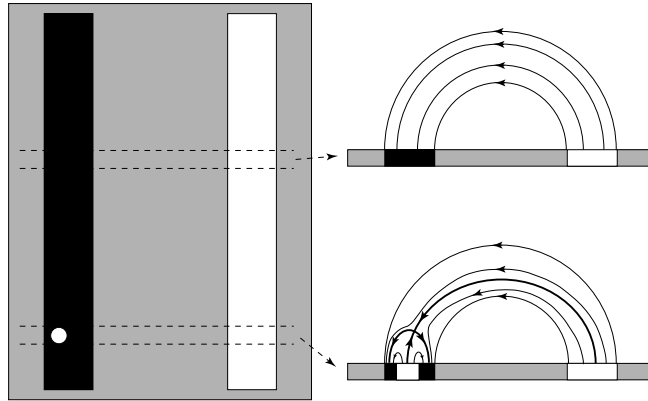


Figure 8. Schematic magnetic field model of the event. Black and white indicate negative and positive polarities, and gray means neutral polarity. The quasi-vertical current sheet above the arcade is not shown here (see Figure 9).

precursor reconnection. However, the arcade loops formed in a simple bipolar configuration (see Figure 8), without changes in their magnetic field structure.

Table 2. Decay times (measured in minutes) of the precursor structure and the loops of the arcade.

Event	Precursor	Loop 1	Loop 2	Loop 3	Loop 4	Loop 5
1	4.5	19	21	36	32	31
2	6.6	21	24	24	—	—
3	4.2	24	23	21	—	—
4	5.4	16	19	24	10	—

Second, the arcades formed in a wave-like manner, which indicates that waves might play a role in the phenomena. Third, there was a cold space (distance) between the hot loops. It is unclear why some loops of the arcade were heated and some were not. Neither the wave-like formation nor the cold space can be explained by the standard 2.5D flare model. We need an extension of the standard flare model into 3D, which will explain the observations.

To explain the observations, we propose that the current sheet existed above the loop apexes before the arcades ignited (see Figure 9). We think that the arcade evolution was the following:

- i) The precursor structure was formed at the edge of the arcade (see Figure 9a).
- ii) The precursor launched an MHD wave, which propagated along the arcade (see Figure 9b).
- iii) The MHD wave caused instabilities in the current sheet (see Figure 9c).
- iv) The instabilities led to the heating of the underlying loops (see Figure 9d).

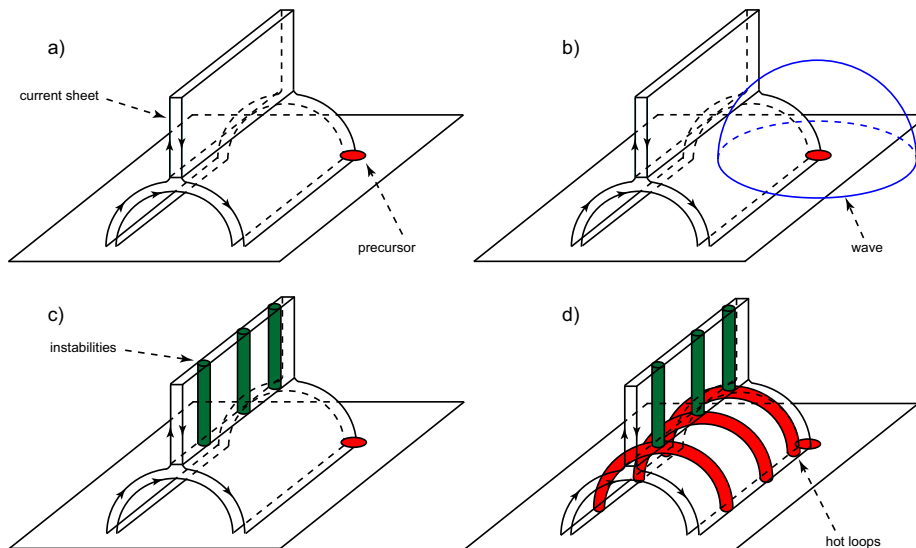


Figure 9. Schematic model of hot loop arcade formation.

Artemyev and Zimovets (2012) studied the unstable wave modes of a quasi-vertical 2.5D current sheet above an arcade with a sheared magnetic field. The studied waves propagated in the current sheet along the PIL. The development of the symmetrical sausage-mode waves to the local thinning and thickenings of the current sheet. Due to the conservation of magnetic flux, the current density is higher where the current sheet is thinner. This process intensifies the tearing instability (Lapenta and Brackbill, 2000; Wiegmann and Büchner, 2000; Lapenta, 2003) and modulates the efficiency of the energy release along the current sheet. Thus, the propagation of the unstable wave modes can lead to successive episodes of plasma heating in different loops of the arcade.

The characteristic distance between the two most effectively heated neighboring loops should approximately be equal to the wavelength (λ) of the corre-

sponding unstable wave mode. The characteristic speed of the triggering front propagating along the PIL should correspond to the group speed of the wave (v_g). The most appropriate unstable wave mode for the flaring loop arcades has the group speed (Artemyev and Zimovets, 2012)

$$v_g \approx \frac{v_A}{4} \sqrt{\frac{\lambda}{L_x}} \sin \varphi, \quad (2)$$

where v_A is the Alfvén speed outside of the current sheet, L_x is the vertical scale of the current sheet, and φ is the shear angle.

Let us apply this theory to the observations. The impulsive energy release during the precursor process could initiate the unstable wave modes in the current sheet above the arcades. Artemyev and Zimovets (2012) predicted that the wavelength lies in the range from 0.1 Mm to 1000 Mm. The observed value $\lambda \approx 50$ Mm corresponds to the collisionless mode 3 found in Artemyev and Zimovets (2012). From the observations, we estimate that $v_g \approx 700$ km s⁻¹ and $\varphi \approx 30^\circ$ (see Figure 2). Thus, to satisfy Equation (2), L_x should be

$$L_x \approx 3 \times 10^{-3} v_A^2 \text{ km} \quad (3)$$

Here, the Alfvén speed v_A is in km s⁻¹. For the estimation, we used the ‘canonical’ value for the solar corona ($v_A = 1000$ km s⁻¹) and found that in the studied events $L_x \approx 3$ Mm. This length is similar to what was found by Reid, Vilmer, and Kontar (2011) in their analysis of the coronal type III radio bursts. Finally, the estimated vertical length of the current sheet is 6 – 7 orders of magnitude greater than the characteristic ion gyroradius in the solar corona (current sheet width), which is a favorable condition for magnetic reconnection and plasma heating.

Let us discuss other possible models. Emslie (1981) proposed that an increase in plasma pressure can increase the cross section of a hot flare loop. The hot loop will interact with a neighboring cold loop of the arcade and cause magnetic reconnection and heating in the cold loop. This process can propagate along the arcade like a domino effect. However, this mechanism cannot explain the cold space between the hot loops.

Nakariakov and Zimovets (2011) proposed that a slow magnetoacoustic wave that propagate along the arcade can trigger energy release in the current sheet above the arcade. The main difference with the model of Artemyev and Zimovets (2012) is the nature of the wave. In the model of Artemyev and Zimovets (2012) the wave propagates inside the current sheet, while in the model of Nakariakov and Zimovets (2011) the wave propagates along the arcade outside the current sheet. In our observations, a group of slow magnetoacoustic waves could be initiated by the precursor. The model of Nakariakov and Zimovets (2011) can explain the wave-like formation of a hot arcade, but it cannot easily explain the cold space between the hot loops.

Liu, Alexander, and Gilbert (2009) analyzed the flares in which a filament erupted asymmetrically along the PIL. In these events, the arcade should brighten in a wave-like manner. Although filaments can erupt several times in a row from

the same active region (Archontis, Hood, and Tsinganos, 2014), the model fails to explain the cold space between the hot loops.

The model of Artemyev and Zimovets (2012) explains both the wave-like formation of the arcades and the cold space between the hot loops. The model gives a reasonable estimate of the current sheet vertical scale. The observed distance between the hot loops is consistent with the model. The Artemyev and Zimovets (2012) model fits our observations better than other models known to us. We hope that the reported observations will stimulate new theoretical investigations and observations of this type of solar flare phenomenon.

5. Conclusions

We presented the first observations of the formation of hot loop arcades in the hot monochromatic line. Thanks to the relatively high cadence of the Mg XII spectroheliograph, we saw the formation of the arcades in detail. At first, a small source of soft X-ray and hard X-ray emissions appeared at the edge of the future arcade. Then the arcade brightened in a wave-like manner. The wave speed was about 700 km s^{-1} , which is the same order of magnitude as the MHD coronal wave speed. The arcades occurred four times in a row in the same place under the same conditions, following the same scenario.

We interpreted the observations in terms of the MHD waves. We think that the current sheet existed above the loop apexes before the arcade ignited. The precursor launched an MHD wave, which triggered instabilities in the current sheet. The instabilities led to the reconnection and loop heating.

Our interpretation is consistent with previous theoretical works (Somov and Syrovatskii, 1982; Artemyev and Zimovets, 2012). The observations show that flares are essentially a 3D processes 2D models do not explain all their aspects. The observations also point out that MHD waves could play an important role in flare processes; they could transfer energy and trigger reconnection.

Acknowledgments We are grateful to Boris Somov and Anton Artemyev for their invaluable help. This work was supported by a grant from the Russian Foundation of Basic Research (grant 14-02-00945) and by the Program No. 22 for fundamental research of the Presidium of the Russian Academy of Sciences.

Appendix

Cooling times

The loops of the arcade kept their high temperature for a long time (see Figure 6). This could be interpreted as a sign of the continuous loop heating. To verify this conclusion, we here estimate the plasma cooling time in the absence of heating, and compare it with the measured values.

There are two mechanisms of loop cooling: conductive and radiative. At high temperatures ($\approx 10 \text{ MK}$), the conductive cooling dominates radiative cooling.

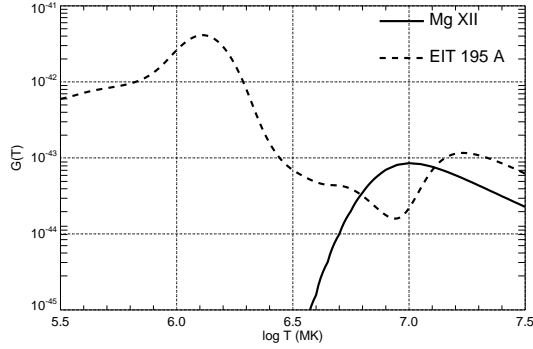


Figure 10. Temperature response functions of the Mg XII spectroheliograph (solid line) and EIT 195 Å telescope (dashed line).

To estimate the conductive cooling time (τ_{cond}), we use the formula (Culhane *et al.*, 1994)

$$\tau_{\text{cond}} = \frac{21n_e k_B L^2}{5\kappa T^{5/2}}, \quad (4)$$

where $\kappa = 9.2 \times 10^{-7} \text{ erg s}^{-1} \text{ cm}^{-1} \text{ K}^{-7/2}$ is the Spitzer conductivity, n_e is the electron density, k_B is the Boltzmann constant, L is the loop length, and T is the loop temperature.

To estimate the arcade temperature, we compared Mg XII and EIT 195 Å images. The EIT 195 Å channel is sensitive to 1 MK and 16 MK plasma (see Figure 10). The Mg XII spectroheliograph is sensitive to plasmas hotter than 5 MK (see Figure 10). Since we see the precursor structure in both EIT 195 Å and Mg XII channels, the precursor temperature should be about 15 MK. Since we were able to see the arcade in the Mg XII line but not in the EIT images, the loop temperature should lie in the range of 5 – 10 MK.

To estimate the precursor electron density, we estimated its temperature (T) and emission measure (EM) under isothermal approximation using the filter ratio method with EIT 195 Å and Mg XII fluxes. The result is $T \approx 14 \text{ MK}$ and $\text{EM} \approx 8.8 \cdot 10^{46} \text{ cm}^{-3}$. The precursor structure had a length of $L \approx 20 \text{ Mm}$ and the width of the EIT pixel. However, since loops in the AIA images have the width of the AIA pixel ($r = 0.44 \text{ Mm}$), we think that the AIA pixel size is a more reasonable estimate for the loop width than the EIT pixel size. Now, we can estimate the precursor electron density:

$$\text{EM} = n_e^2 \pi r^2 L \Rightarrow n_e = \sqrt{\frac{\text{EM}}{\pi r^2 L}} \approx 8.6 \cdot 10^{10} \text{ cm}^{-3}. \quad (5)$$

Unfortunately, we have only Mg XII observations for the flaring loops, so that there is no way to measure the emission measure and temperature of their plasma separately using the filter ratio. However, we can estimate their electron density from

$$I = G(T)n_e^2\pi r^2L \leq G_{\max}n_e^2\pi r^2L, \quad (6)$$

namely,

$$n_e \geq \sqrt{\frac{I}{G_{\max}\pi r^2L}} \approx 1.8 \cdot 10^{10} \text{ cm}^{-3}, \quad (7)$$

where I is the emission intensity of the loops on the Mg XII images, $G(T)$ is the temperature response function of the Mg XII spectroheliograph, and G_{\max} is the maximum value of $G(T)$. For the sake of estimation, we used $n_e = 10^{10} \text{ cm}^{-3}$ and $T = 10 \text{ MK}$ for the loops of the arcade.

For the loops, we obtained $\tau_{\text{cond}} = 100 \text{ min}$ ($n_e = 10^{10} \text{ cm}^{-3}$, $T = 10 \text{ MK}$, and $L = 170 \text{ Mm}$). This is of the same order of magnitude as the measured values, 20 – 30 min. Furthermore, slight changes of the n_e and T values can make the agreement better. This means that it is possible that the loop heating was impulsive and long lifetime of the loops was due to their large size.

For the precursor, we obtained $\tau_{\text{cond}} = 5 \text{ min}$ ($n_e = 8.6 \cdot 10^{10} \text{ cm}^{-3}$, $T = 14 \text{ MK}$, and $L = 20 \text{ Mm}$), which coincides with the observed values. This means that it is possible that the heating of the precursor structure was impulsive.

It may be surprising that the long decay of the Mg XII light curves can be interpreted as pure cooling. However, our estimate is very rough; it is valid in the temperature range $6.8 < \log T < 7.3$, where the response function of Mg XII channel does not change much. Therefore, pure cooling is only an option, but not a fact.

Furthermore, other mechanisms could decrease the loop intensity; for example by mass draining. The mass draining could play a significant role in the late phase of flare decay (Bradshaw and Cargill, 2010). The draining will decrease the electron density, and therefore the loop intensity will decrease faster. Also, according to Equation (4), the loops will cool faster. If the draining was present, then the hot loops would require continuous heating to support their long decay times.

References

- Archontis, V., Hood, A.W., Tsinganos, K.: 2014, Recurrent explosive eruptions and the “sigmoid-to-arcade” transformation in the Sun driven by dynamical magnetic flux emergence. *Astrophys. J. Lett.* **786**, L21. DOI. ADS.
- Artemyev, A., Zimovets, I.: 2012, Stability of current sheets in the solar corona. *Solar Phys.* **277**, 283. DOI. ADS.
- Benz, A.O.: 2008, Flare observations. *Living Rev. in Solar Phys.* **5**(1). DOI. <http://www.livingreviews.org/lrsp-2008-1>.
- Bogachev, S.A., Somov, B.V., Kosugi, T., Sakao, T.: 2005, The motions of the hard X-ray sources in solar flares: Images and statistics. *Astrophys. J.* **630**, 561. DOI. ADS.
- Bradshaw, S.J., Cargill, P.J.: 2010, The cooling of coronal plasmas. III. Enthalpy transfer as a mechanism for energy loss. *Astrophys. J.* **717**, 163. DOI. ADS.
- Carmichael, H.: 1964, A process for flares. In: Ness, W.N. (ed.) *AAS-NASA Symposium on the Physics of Solar Flares, NASA SP-50*, 451. ADS.
- Culhane, J.L., Phillips, A.T., Ina-Koide, M., Kosugi, T., Fludra, A., Kurokawa, H., Makishima, K., Pike, C.D., Sakao, T., Sakurai, T.: 1994, YOHKOH observations of the creation of high-temperature plasma in the flare of 16 December 1991. *Solar Phys.* **153**, 307. DOI. ADS.

-
- Delaboudinière, J., Artzner, G.E., Brunaud, J., Gabriel, A.H., Hochedez, J.F., *et al.*: 1995, EIT: Extreme-Ultraviolet Imaging Telescope for the SOHO mission. *Solar Phys.* **162**, 291. DOI. ADS.
- Domingo, V., Fleck, B., Poland, A.I.: 1995, The SOHO mission: An overview. *Solar Phys.* **162**, 1. DOI. ADS.
- Emslie, A.G.: 1981, An interacting loop model for solar flare bursts. *Astrophys. J. Lett.* **22**, 41. ADS.
- Fletcher, L., Dennis, B.R., Hudson, H.S., Krucker, S., Phillips, K., Veronig, A., *et al.*: 2011, An observational overview of solar flares. *Space Sci. Rev.* **159**, 19. DOI. ADS.
- Golub, L., Deluca, E., Austin, G., Bookbinder, J., Caldwell, D., Cheimets, P., *et al.*: 2007, The X-Ray Telescope (XRT) for the Hinode mission. *Solar Phys.* **243**, 63. DOI. ADS.
- Grigis, P.C., Benz, A.O.: 2005, The spectral evolution of impulsive solar X-ray flares. II. Comparison of observations with models. *Astron. Astrophys.* **434**, 1173. DOI. ADS.
- Hirayama, T.: 1974, Theoretical model of flares and prominences. I: Evaporating flare model. *Solar Phys.* **34**, 323. DOI. ADS.
- Jing, J., Lee, J., Liu, C., Gary, D.E., Wang, H.: 2007, Hard X-ray intensity distribution along $H\alpha$ ribbons. *Astrophys. J. Lett.* **664**, L127. DOI. ADS.
- Kopp, R.A., Pneuman, G.W.: 1976, Magnetic reconnection in the corona and the loop prominence phenomenon. *Solar Phys.* **50**, 85. DOI. ADS.
- Krucker, S., Hudson, H.S., Jeffrey, N.L.S., Battaglia, M., Kontar, E.P., Benz, A.O., Csillaghy, A., Lin, R.P.: 2011, High-resolution imaging of solar flare ribbons and its implication on the thick-target beam model. *Astrophys. J.* **739**, 96. DOI. ADS.
- Lapenta, G.: 2003, A new paradigm for 3D collisionless magnetic reconnection. *Space Sci. Rev.* **107**, 167. DOI. ADS.
- Lapenta, G., Brackbill, J.U.: 2000, 3D reconnection due to oblique modes: a simulation of harris current sheets. *Nonlinear Proc. in Geophys.* **7**, 151. DOI. <http://www.nonlin-processes-geophys.net/7/151/2000/>.
- Lemen, J.R., Title, A.M., Akin, D.J., Boerner, P.F., Chou, C., Drake, J.F., *et al.*: 2011, The Atmospheric Imaging Assembly (AIA) on the Solar Dynamics Observatory (SDO). *Solar Phys.*, 172. DOI. ADS.
- Lin, R.P., Dennis, B.R., Hurford, G.J., Smith, D.M., Zehnder, A., Harvey, P.R., *et al.*: 2002, The Reuven Ramaty High-Energy Solar Spectroscopic Imager (RHESSI). *Solar Phys.* **210**, 3. DOI. ADS.
- Liu, C., Lee, J., Yurchyshyn, V., Deng, N., Cho, K.S., Karlický, M., Wang, H.: 2007, The eruption from a sigmoidal solar active region on 2005 May 13. *Astrophys. J.* **669**, 1372. DOI. ADS.
- Liu, R., Alexander, D., Gilbert, H.R.: 2009, Asymmetric eruptive filaments. *Astrophys. J.* **691**, 1079. DOI. ADS.
- Masuda, S., Kosugi, T., Hudson, H.S.: 2001, A hard X-ray two-ribbon flare observed with Yohkoh/HXT. *Solar Phys.* **204**, 55. DOI. ADS.
- McLaughlin, J.A., Hood, A.W., de Moortel, I.: 2011, Review article: MHD wave propagation near coronal null points of magnetic fields. *Space Sci. Rev.* **158**, 205. DOI. ADS.
- Nakariakov, V.M., Zimovets, I.V.: 2011, Slow magnetoacoustic waves in two-ribbon flares. *Astrophys. J. Lett.* **730**, L27. DOI. ADS.
- Nakariakov, V.M., Foullon, C., Verwichte, E., Young, N.P.: 2006, Quasi-periodic modulation of solar and stellar flaring emission by magnetohydrodynamic oscillations in a nearby loop. *Astron. Astrophys.* **452**, 343. DOI. ADS.
- Oraevsky, V.N., Sobelman, I.I.: 2002, Comprehensive studies of solar activity on the CORONAS-F satellite. *Astron. Lett.* **28**, 401. DOI. ADS.
- Parenti, S., Reale, F., Reeves, K.K.: 2010, Post-flare evolution of AR 10923 with Hinode/XRT. *Astron. Astrophys.* **517**, A41. DOI. ADS.
- Reale, F., Guarrasi, M., Testa, P., DeLuca, E.E., Peres, G., Golub, L.: 2011, Solar Dynamics Observatory discovers thin high temperature strands in coronal active regions. *Astrophys. J. Lett.* **736**, L16. DOI. ADS.
- Reid, H.A.S., Vilmer, N., Kontar, E.P.: 2011, Characteristics of the flare acceleration region derived from simultaneous hard X-ray and radio observations. *Astron. Astrophys.* **529**, A66. DOI. ADS.
- Reva, A., Shestov, S., Bogachev, S., Kuzin, S.: 2012, Investigation of hot X-ray points (HXPs) using spectroheliograph Mg XII experiment data from CORONAS-F/SPIRIT. *Solar Phys.* **276**, 97. DOI. ADS.

-
- Scherrer, P.H., Bogart, R.S., Bush, R.I., Hoeksema, J.T., Kosovichev, A.G., Schou, J., *et al.*: 1995, The Solar Oscillations Investigation - Michelson Doppler Imager. *Solar Phys.* **162**, 129. DOI. ADS.
- Somov, B.V., Syrovatskii, S.I.: 1982, Thermal trigger for solar flares and coronal loops formation. *Solar Phys.* **75**, 237. DOI. ADS.
- Sturrock, P.A.: 1966, Model of the high-energy phase of solar flares. *Nature* **211**, 695. DOI. ADS.
- Testa, P., Reale, F.: 2012, Hinode/EIS spectroscopic validation of very hot plasma imaged with the Solar Dynamics Observatory in non-flaring active region cores. *Astrophys. J. Lett.* **750**, L10. DOI. ADS.
- Tripathi, D., Isobe, H., Mason, H.E.: 2006, On the propagation of brightening after filament/prominence eruptions, as seen by SoHO-EIT. *Astron. Astrophys.* **453**, 1111. DOI. ADS.
- Tsuneta, S., Acton, L., Bruner, M., Lemen, J., Brown, W., Carvalho, R., Catura, R., Freeland, S., Jurcevic, B., Owens, J.: 1991, The soft X-ray telescope for the SOLAR-A mission. *Solar Phys.* **136**, 37. DOI. ADS.
- Urnov, A.M., Shestov, S.V., Bogachev, S.A., Goryaev, F.F., Zhitnik, I.A., Kuzin, S.V.: 2007, On the spatial and temporal characteristics and formation mechanisms of soft X-ray emission in the solar corona. *Astron. Lett.* **33**, 396. DOI. ADS.
- Vorpahl, J.A.: 1976, The triggering and subsequent development of a solar flare. *Astrophys. J.* **205**, 868. DOI. ADS.
- Warren, H.P., Winebarger, A.R., Brooks, D.H.: 2012, A systematic survey of high-temperature emission in solar active regions. *Astrophys. J.* **759**, 141. DOI. ADS.
- Warren, H.P., Bookbinder, J.A., Forbes, T.G., Golub, L., Hudson, H.S., Reeves, K., Warshall, A.: 1999, TRACE and Yohkoh observations of high-temperature plasma in a two-ribbon limb flare. *Astrophys. J. Lett.* **527**, L121. DOI. ADS.
- Wiegmann, T., Büchner, J.: 2000, Kinetic simulations of the coupling between current instabilities and reconnection in thin current sheets. *Nonlinear Proc. in Geophys.* **7**, 141. DOI. <http://www.nonlin-processes-geophys.net/7/141/2000/>.
- Zhitnik, I.A., Bougaenko, O.I., Delaboudiniere, J.-P., Ignatiev, A.P., Korneev, V.V., Krutov, V.V., *et al.*: 2002, SPIRIT X-ray telescope/spectroheliometer results. In: Wilson, A. (ed.) *Solar Variability: From Core to Outer Frontiers*, ESA SP-506, 915. ADS.
- Zhitnik, I.A., Bougaenko, O.I., Ignat'ev, A.P., Krutov, V.V., Kuzin, S.V., Mitrofanov, A.V., *et al.*: 2003, Dynamic 10 MK plasma structures observed in monochromatic full-Sun images by the SPIRIT spectroheliograph on the CORONAS-F mission. *Mon. Not. Roy. Astron. Soc.* **338**, 67. DOI. ADS.